MICROSTRUCTURAL CHANGES IN HOMOGENIZED TWIN-ROLL CAST Al-Mg-Si ALLOY

MILOŠ JANEČEK[1]*, MARGARITA SLÁMOVÁ[2], MIROSLAV CIESLAR[1]

Age-hardenable Al-Mg-Si aluminium alloys (AA6xxx series) are used for car body applications where high formability and in-service strength are major requirements. One of the mostly used materials for such applications in Europe is currently the low Cu content AA6016 alloy, which contains approximately 0.4 wt.% of Mg and 1.0 wt.% of Si. The strengthening phase in this alloy is Mg_2Si in the form of small semi-coherent precipitates. Direct chill (DC) cast alloys are currently used in automotive skin panels and have been extensively studied during last years. Recently, the new technology of twin-roll casting (TRC) offered an alternative way of sheet manufacturing for automotive applications. In this paper, the influence of homogenization annealing on the mechanical response and microstructure evolution of a TRC AA6016 alloy was studied.

K e y w o r d s: aluminium alloys, twin-roll casting, microstructure evolution, precipitation hardening

MIKROSTRUKTURNÍ ZMĚNY V HOMOGENIZOVANÉ SLITINĚ Al-Mg-Si PŘIPRAVENÉ METODOU PLYNULÉHO LITÍ

Tepelně zpracovatelné hliníkové slitiny Al-Mg-Si (série AA6xxx) nalézají stále větší použití v automobilovém průmyslu při výrobě vnějších plechů karoserie, kdy je požadována vysoká tvárnost a provozní pevnost. Jedním z nejčastěji používaných materiálů pro tyto aplikace je v současné době slitina AA6016 s nízkým obsahem Cu, která běžně obsahuje 0,4 hm.% Mg and 1,0 hm.% Si. Svou pevnost získává díky precipitaci drobných semikoherentních částic fáze Mg_2Si. V posledních letech byly významně studovány slitiny připravené metodou přímého lití do kokil (DC casting). Nedávno se objevila nová technologie plynulého lití mezi válce (TRC – twin-roll casting), jako alternativní metoda

[1] Department of Metal Physics, Charles University, Ke Karlovu 5, 121 16 Prague 2, Czech Republic
[2] Research Institute for Metals Panenské Břežany, Ltd., Panenské Břežany 50, 250 70 Odolena Voda, Czech Republic
* corresponding autor, e-mail: `janecek@met.mff.cuni.cz`

výroby velkých plechů pro aplikace v automobilovém průmyslu. V tomto článku je studován vliv homogenizačního žíhání na mechanické vlastnosti a vývoj mikrostruktury ve slitině AA6016 připravené technologií plynulého lití.

1. Introduction

The growing demand of fuel-efficient vehicles to reduce energy consumption and thus, to decrease environment pollution, has led to increased interest in sheets made from aluminium alloys to respond to weight reduction demand of automotive industry [1, 2]. Some of the intrinsic properties of aluminium such as high strength to weight ratio, good formability, good corrosion resistance and recycling potential make it the ideal candidate to replace heavier materials (steel) in cars. In this regard, the interest in age-hardenable AA6xxx series alloys has significantly increased in the last years [3–5]. These alloys achieve their final strength during the paint bake cycle, which is usually the last procedure of car manufacturing. Therefore, the sheets from these alloys should meet two principal requirements imposed by the needs of skin panel stamping and car life-cycle performance. The sheets should exhibit: i) a relatively low strength in the as-delivered condition T4 (solution heat treated and naturally aged) or T4P (stabilized [6]) to provide sufficient formability to make the part; ii) a high strength in the part after final painting – T8X temper [7]. The alloys AA6009, AA6010, AA6016 and AA6111 are among the alloys used for car body sheets [8].

The current technology for the production of AA6xxx sheets is based on direct chill (DC) casting and involves several processes: i) DC casting; ii) preheating at temperatures between 480–580 ℃ to reduce short range intercellular segregation (coring) and to dissolve soluble phases; iii) two stage hot rolling to thickness between 3 and 6 mm; iv) cold rolling to the final thickness of 0.8–1.2 mm; v) solution treating at temperatures between 500 and 570 ℃ to dissolve hardening phases followed by a quench to retain corresponding alloying elements in solid solution.

Alloy microstructure evolution during thermo-mechanical processing of DC cast AA6xxx series alloys has been extensively studied. Details can be found in the review [7], while details on ageing behaviour and precipitation hardening in [5, 6, 9].

The decomposition of the supersaturated solid solution (SSS) of age hardenable Al-Mg-Si alloys has been extensively studied and is believed to proceed in the following sequence [9, 10]:

$$\mathrm{SSS} \rightarrow (\mathrm{Mg}+\mathrm{Si})\ \mathrm{clusters/GP(I)}_{\mathrm{platelike,\ spherical}} \rightarrow \beta''/\mathrm{GP(II)}_{\mathrm{needles}} \rightarrow \\ \rightarrow \beta'_{\mathrm{rods}} \rightarrow \beta_{\mathrm{plates}}.$$

The decomposition process begins with the formation of two types of (Mg + Si) clusters – Si rich (Mg + Si) cluster, which is then enriched by the diffusion of Mg atoms to form the Si-depleted plate-like or spherical (Mg + Si) clusters or GP(I) zone. As ageing proceeds clusters and zones become ordered and develop the needle shaped GP(II)/β'' phase. These precipitates are needle shaped and aligned along $\langle 100\rangle_{\mathrm{Al}}$ axis. They range between 20–100 nm in length, are approximately 6 nm in diameter and are the predominant phase in the peak-aged state [11]. Their crystallographic structure has not yet been unambiguously determined. β' precipitates form after β'' precipitates in the ageing sequence. They are rod shaped and aligned along $\langle 100\rangle_{\mathrm{Al}}$ axis. Their crystallographic structure was determined by Cayron and Buffat only recently [12]. These particles have hexagonal structure and belong to the space group P-620. The final step of the precipitation sequence is the equilibrium β-Mg_2Si phase which has the form of platelets lying in $\{100\}_{\mathrm{Al}}$ planes. Their structure has been well characterized as the FCC CaF_2 type with $a = 0.64$ nm [13]. However, these particles contribute only little to the strength of the alloy.

Although DC-casting based manufacturing of automotive sheets is nowadays well established, ways to improve its economy are looked for. The production of Al sheet by the twin-roll continuous (TRC) casting, rather than by the conventional DC casting and hot rolling route, offers an opportunity to substantially reduce sheet cost. Continuous casting requires lower capital, has low production-cycle energy consumption and low manufacturing costs. For this reason, manufacturing of automotive sheets by TRC casting is highly challenging and works in this field have already started [14]. TRC casting has proved its advantage in the production of packaging foils and materials for heat exchangers (finstock). Recently we have performed detail studies of structural transformations in TRC Al-Fe-Mn-Si alloy (AA8006) finstock materials [15, 16]. The casting of AA6016 alloy by the TRC methods is a brand new technology. There is very little information on the physical and metallurgical aspects of the production of such materials. Detail investigation of the thermo-mechanical processing of TRC AA6xxx is necessary in order to optimize the manufacturing process and sheet properties. In this paper, the result of a study aimed at understanding the response of a TRC AA6016 alloy to high temperature (homogenization) annealing is reported.

2. Experimental

The alloy AA6016 used in this investigation was provided by ASSAN Turkey. The alloy was cast on a speed twin-roll caster. The chemical composition of the alloy is given in Table 1. The amount of excess Si was calculated taking into account the following facts: i) Si and Mg atoms have a strong mutual affinity and form the Mg_2Si compound, in which Si : Mg weight ratio equals to 1.73; ii) due to low iron solubility in Al, ternary Al-Fe-Si compounds form in commercial Al alloy at casting; iii) the amount of Si in these compounds was calculated assuming that the whole Fe content was consumed and Si : Fe ratio in these particles is 1 : 5 [5]. The excess Si in the alloy under investigation is 0.64 wt.%. The as-cast sheets of the thickness of 5.8 mm were cold rolled on a laboratory mill to the thickness of 3.7 mm (36% reduction, $\varepsilon \sim 0.52$). The sheets were then homogenized at low and

Table 1. Chemical composition of AA6016 alloy used in the study

Element	Mg	Mn	Fe	Si	Cu	Ti	Cr	Zn
wt.%	0.47	0.066	0.14	0.95	0.0061	0.028	< 0.0009	0.0065

high temperature of 500 ℃ and 550 ℃, respectively. The details of both homogenization procedures are given in Table 2. The laboratory homogenization simulated the industrial procedure, in which large coils of TRC sheets are annealed in chamber furnaces. This procedure involves very long heating and cooling times. Vickers hardness HV 10 and conductivity κ was measured before and after homogenization in order to assess the rate of softening and global changes in Al solid solution content. Moreover, samples quenched in cold water after the soaking at both temperatures were analysed. The natural ageing was studied only by means of hardness and conductivity measurements. Light microscopy examinations were carried out on samples cut parallel to the normal (ND) and rolling (RD) directions, grinded and polished in a conventional manner. Grain structure was examined on samples anodized in Barkers reagent (solution of fluoroborid acid in water) using crossed polarizers. Thin foils for transmission electron microscopy (TEM) were prepared by electropolishing in a 30% HNO_3 in methanol solution at -17 ℃ using Tenupol twin jet device. TEM investigations were carried out with a JEOL 2000 FX electron microscope operated at 200 kV. Phase composition of individual particles was analysed using an EDAX X-ray analyser hooked up to the electron microscope Philips CM200 operated at 200 kV.

3. Results and discussion

3.1 Light microscopy observation

Light microscopy examinations of as-cast samples showed the presence of coarse segregation clusters in the central plane of the sheets, so called Centre-line segregation channels (CLSC – Fig. 1a). Outside CSLC, the primary second-phase compounds in small eutectic colonies were found. Micro-segregation of solute elements (coring) was observed at large magnifications in as-cast dendrites (Fig. 1b). The grains in the as-cast material are elongated in the casting/rolling direction and having the size of 96 μm in the rolling and 36 μm in the normal direction, respectively (Table 3). Cold rolling resulted in flattening of grain structure, elongation of segregation and eutectic clusters. Deformation bands were observed in many areas, which are supposed to represent band of localized deformation (Lüders bands – Fig. 2a).

The homogenization treatment at both temperatures has a two-fold effect. It results in second-phase particle transformation and in recrystallization. Melted particles of the low-melting Al_3Mg_2 compound were occasionally observed in CLSC.

Table 2. Designation and treatment of samples used in the study

Sample	Treatment	Thickness [mm]	Reduction [%]	True deformation
N6	as-cast	5.83	0	0
N4	rolled	3.71	36.4	0.52
N4L	homog./500 ℃	3.71	36.4	0.52
N4H	homog./550 ℃	3.71	36.4	0.52

Sample N4L		
	Total time [h]	T [℃]
Heating	0	25
	4	230
	8	350
	13	450
	18	500
Hold	28	**500**
Cooling	29	430
	32	280
	38	100

Sample N4H		
	Total time [h]	T [℃]
Heating	0	25
	4	230
	8	350
	13	450
	23	550
Hold	29	**550**
Cooling	31	400
	34	250
	39	100

Table 3. Grain size and shape of as-cast and homogenized samples (L – rolling direction, S – normal direction, SD – standard deviation)

	T_{H}	$\overline{L}$ [μm]		$SD(\overline{L})$		Shape
Sample	[℃]	dir. L	dir. S	dir. L	dir. S	L/S
N6 (as-cast)	–	96	36	6.2	4.4	2.7
N4L-center	500	53	28	4.4	3.0	1.9
N4H-center	550	58	31	6.9	1.6	1.9
N4L-surface	500	52	23	4.8	1.9	2.3
N4H-surface	550	52	24	3.9	1.3	2.2

Inside and outside clusters of coarse particles, the transformation resulted in coarsening and/or coagulation of the constituents of CLSC and eutectic colonies. Many tiny particles, probably coarsened Mg_2Si precipitates were observed. More Mg_2Si precipitates were found in the sample homogenized at 550 ℃ than in the sample homogenized at 500 ℃.

Figures 2b,c show the grain structure of both homogenized samples (their grain size is given in Table 3). The grains in the sample homogenized at 500 ℃ are slightly smaller than in the other sample. In both samples, recrystallized grains at surface are flatter than in the central part of the sheet. This difference in grain

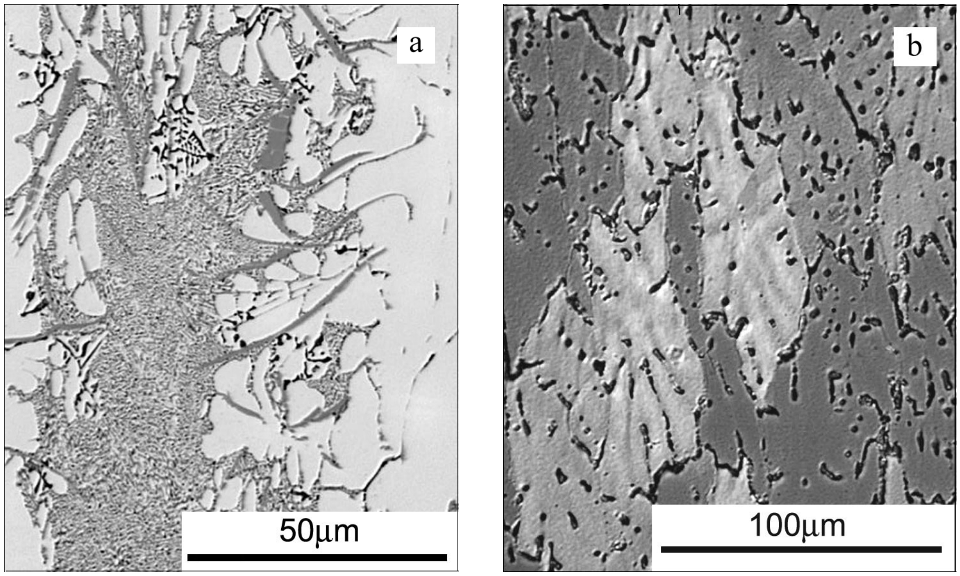

Fig. 1. Light microscopy micrograph of CLSC (a) and grain in the as-cast alloy (b).

shape in the bulk and at the surface may be caused by two facts. Surface layers suffer more intensive deformation (especially of shear type) than the inner parts of sheet volume. Furthermore, many second-phase particles are present (due to higher crystallization rate as compared to the bulk during TRC casting). They are often located on former as-cast grain boundaries, which are also more closely spaced at the surface. Second phase particles exert on the boundaries of new grains strong drag. All these facts could explain the resulting heterogeneity of grain size and shape after homogenization.

3.2 Hardness and conductivity evolution during rolling and homogenization

The results of hardness and conductivity measurements are given in Table 4 and graphically compared in Figs. 3a,b. The table contains the results of samples both quenched in cold water and slow cooled to room temperature after the soaking at 500 °C and 550 °C for 10 h and 5 h, respectively. The hardness, as expected, increases due to cold rolling. On the other hand, after the homogenization treatment, involving slow cooling to room temperature, the hardness decreases significantly, i.e. the alloy did not manifest its potential of age hardening. Hardness decrease as compared to the cold worked state is less significant in the samples quenched after soaking. In this case the soaking plays the role of solution treatment. Natural

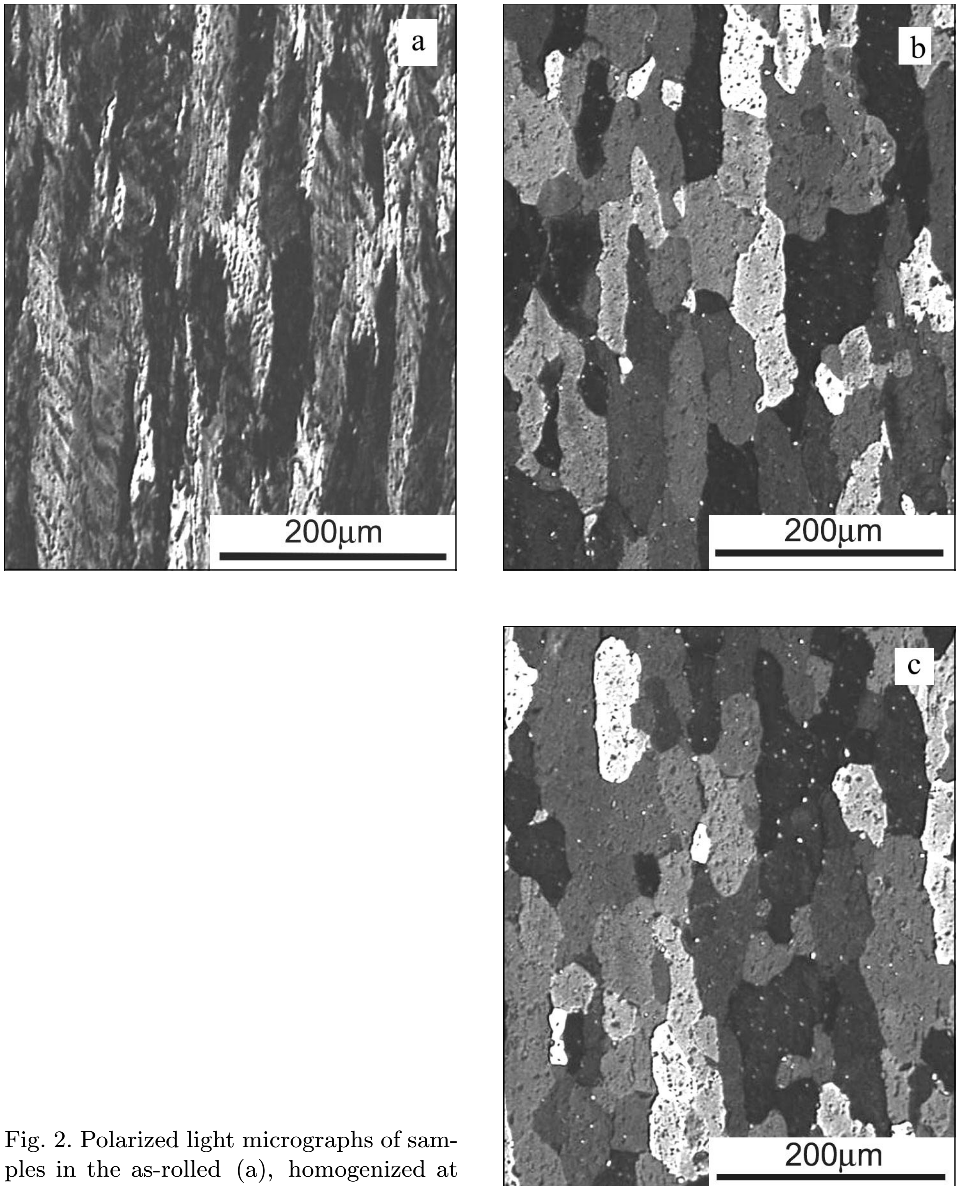

Fig. 2. Polarized light micrographs of samples in the as-rolled (a), homogenized at 500 ℃ (b) and 550 ℃ (c) states.

ageing at room temperature leads to gradual increase in hardness (Fig. 4), which is connected with the precipitation of the hardening phase Mg_2Si. The temperature of soaking affects the magnitude of hardness both in as-quenched and aged samples. Higher hardness is observed in the sample annealed at 550 ℃ than in the sample

T a b l e 4. Hardness (HV 10) and conductivity (κ) of as-cast, rolled, solution treated, aged, and homogenized samples

		HV 10		κ [m·Ω^{-1}·mm^{-2}]
Sample	Condition	mean	SD	mean
N6	as-cast	57.1	1.73	30.0
N4	rolled	69.0	1.50	29.1
N4LQ	500 ℃/quench.	37.8	0.55	28.1
N4L-T4	natural age-hard.	52.5	1.00	27.3
N4L	500 ℃/slow cool.	29.2	0.40	32.7
N4HQ	550 ℃/quench.	41.1	0.35	27.5
N4H-T4	natural age-hard.	58.1	1.00	26.6
N4H	550 ℃/slow cool.	28.1	0.40	31.7

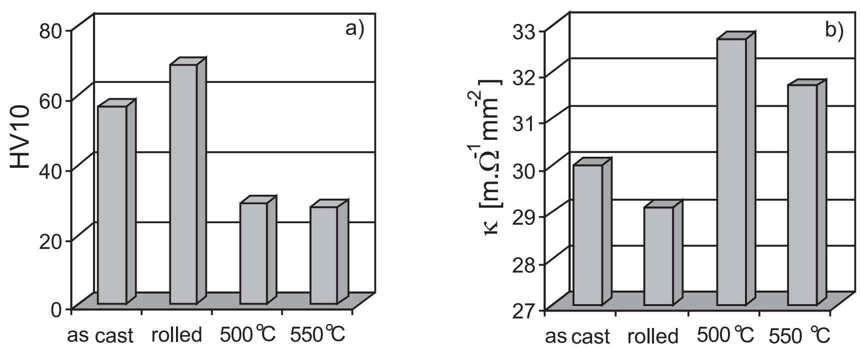

Fig. 3. Hardness (a) and conductivity (b) changes due to rolling (37% reduction), homogenization at 500 ℃ and 550 ℃, respectively.

annealed at 500 ℃. On the other hand, the lower conductivity was measured in the sample annealed at 550 ℃. Both results indicate that the annealing at higher temperature results in higher saturation of the aluminium solid solution with solute atoms of Mg and Si. The natural ageing of the sample treated at 550 ℃ obviously results in higher hardness (Table 4).

3.3 TEM observations

The microstructure of the as-cast alloy (not shown here) is fully recovered comprising well apparent elongated subgrains of approximately 3 μm in diameter. Irregularly shaped (most frequently elongated) primary particles containing Fe and Si with a size of 2–10 μm were mostly found at grain boundaries. This structure is very similar to that of DC cast and hot rolled 6xxx alloys [8].

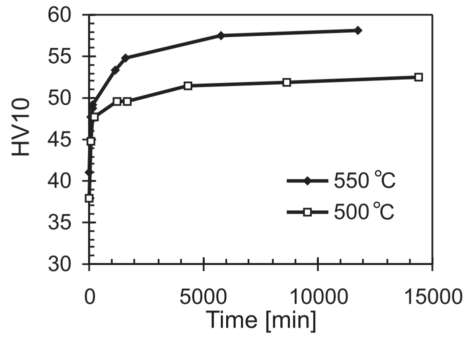

Fig. 4. Time evolution of hardness in samples quenched in water after soaking for 10 h and 5 h at 500 °C and 550 °C, respectively.

The microstructure after cold rolling is shown in Fig. 5. It is a typical cold rolled, deformed, nonrecovered structure. It was observed that some of the coarse primary particles broke up during cold rolling and lost their elongated shape (Fig. 5a). Near these particles, subgrains were often observed and are assumed to be formed as a result of dynamic or postdynamic recovery (Fig. 5b).

The structure of the sample homogenized at lower temperature (500 °C) is fully recovered. Many Mg_2Si precipitates of various morphologies were observed. One example of Mg_2Si particle morphology is shown in Fig. 6, where both metastable precursors of Mg_2Si phase – fine β'' needles and coarser β' rods are seen. Some of these particles point out of the matrix. This confirms that their crystallographic direction is parallel to $\langle 100 \rangle_{\mathrm{Al}}$ (they lie in the direction of the electron beam and Al is etched out in this direction). Mg_2Si precipitates are distributed very heterogeneously. No Mg_2Si particles were found in large areas of the specimen, whereas in some zones their number was relatively high. Besides the Mg_2Si phase, coarse particles of the primary α-$Al_{12}(Mn,Fe)_3Si$ phase of the size of several micrometers were also found in the structure.

A TEM micrograph of the specimen homogenized at 550 °C is in Fig. 7, which shows a fully recrystallized structure containing coarse grains. Relatively homogeneously distributed rods of β'-Mg_2Si precipitates of the length of 1 μm were found. Moreover, many coarse particles (of the average size of several micrometers) were also observed. These coarse particles were identified as α-$Al_{12}(Mn,Fe)_3Si$ phase and $Al_6(Mn,Fe)$, others were complex phase particles containing Mn, Fe, Si and other elements.

TEM investigations of homogenized samples of AA6016 alloy indicate that the temperature influences the precipitation processes occurring during slow cooling. The main differences between samples annealed at low (500 °C, sample N4L) and high (550 °C, sample N4H) temperature can be summarized as follows:

a) The sample annealed at 550 °C contains much more precipitates. This result is in agreement with the results of hardness and conductivity measurements of samples quenched from both temperatures (Table 4).

b) Mg_2Si precipitates were found in both samples. In sample N4L, fine β'' needle-like precursor was found and coarser β' rods were observed only rarely.

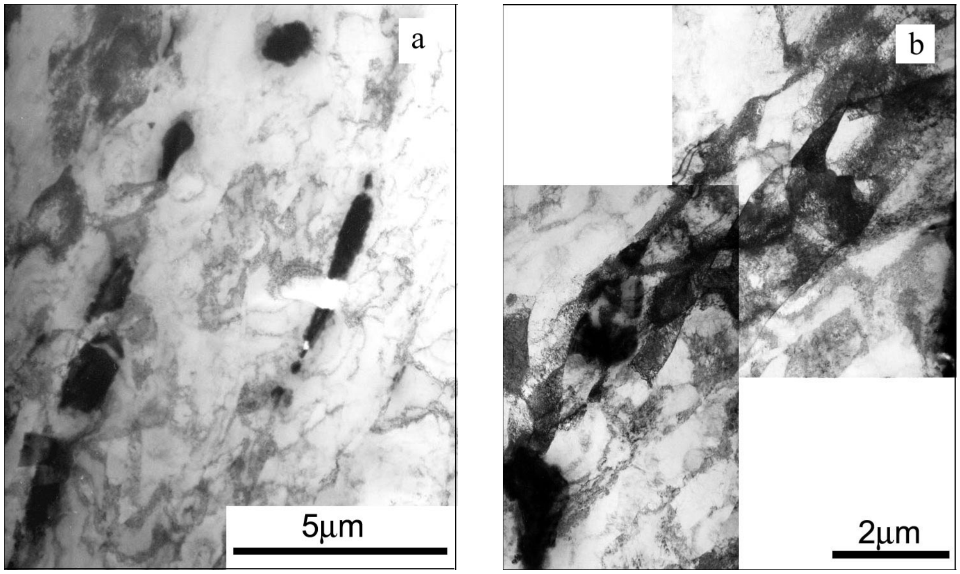

Fig. 5. TEM micrograph of cold rolled structure of the alloy-oval primary phases (a), subgrains (b).

In sample N4H, only β' rods were found. These particles were homogeneously distributed in the matrix of the sample N4H, while in sample N4L they were found in some areas only. Large areas without Mg_2Si particles exist in sample N4L.

c) primary α-$Al_{12}(Mn,Fe)_3Si$ particles were found in both samples. Significantly more particles of this phase were found in sample N4H.

d) Many complex phase particles were found in sample N4H, while in sample N4L these particles were observed only rarely.

4. Summary

Results of the investigation of the changes occurring during the homogenization of a twin-roll cast AA6016 alloy can be summarized as follows:

1. Coarse segregation clusters present in the central plane of the sheets and finely dispersed eutectic colonies transform during homogenization into particles of stable phases. Melting of Al_3Mg_2 particles in CLSC is observed.

2. The homogenization results in recrystallization, precipitation and coarsening of particles of several phases, identified by TEM examinations (see (3)). Homogenization temperature has only small effect on grain size. The grains in the sample homogenized at higher temperature are slightly coarser.

3. The phase composition of the alloy having Si excess of 0.64 wt.% was identified. The samples subjected to homogenization treatment contain coarse primary particles of the α-$Al_{12}(Mn,Fe)_3Si$ phase, occasionally $Al_6(Mn,Fe)$ phase and other

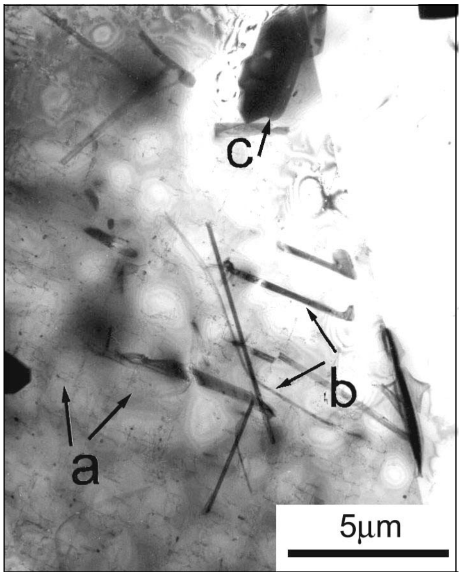

Fig. 6. Mg_2Si precipitates in sample homogenized to 500 ℃: a) fine β'' needles, b) coarser β' rods, c) $Al_{12}(Mn,Fe)_3Si$ particle.

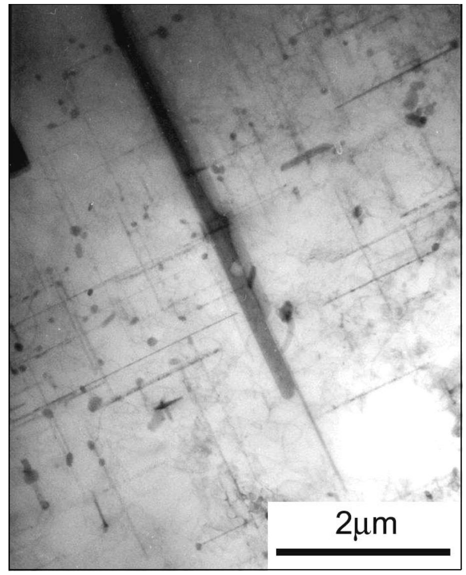

Fig. 7. β'-Mg_2Si rods in sample homogenized to 550 ℃.

complex phase particles. After homogenization, tiny Mg_2Si particles were also observed.

4. The homogenization temperature influences the precipitation as well as the decomposition. In the sample homogenized at 500 ℃ less precipitates and only β''--Mg_2Si needles were found, while in sample homogenized at 550 ℃ more extensive precipitation occurs and mainly β'-Mg_2Si rods were observed.

5. The temperature of homogenization influences also the resulting hardness and the conductivity. The differences of these values in both specimens correlate well with the differences in precipitation. Homogenization at 550 ℃ results in higher solute solution saturation, which consequently leads to the formation of more precipitates upon slow cooling.

6. The temperature of solution treatment influences the hardness of samples quenched and naturally aged for two weeks: annealing at higher temperature results in higher hardness.

Acknowledgements

The authors would like to dedicate this paper to Prof. Dr. Petr Kratochvíl, DrSc., on the occasion of his 70th birthday. The financial support of the Ministry of Education, Youth and Sports of the Czech Republic provided in the framework of the project OE100/E!2530 CASTCALTRANS is gratefully acknowledged.

REFERENCES

[1] ARNOLD, S. A.: J. Metals, *45*, 1993, p. 12.
[2] COLE, G. S.—SHERMAN, A. M.: Mater. Characterization, *35*, 1995, p. 3.
[3] HIRSCH, J.: Mater. Sci. Forum, *242*, 1997, p. 33.
[4] MILLER, W. S.—ZHUANG, L.—BOTTEMA, J.—WITTEBROOD, A. J.—De SMET, P.—HASZLER, A.—VIEREGGE, A.: Mat. Sci. Eng., *A280*, 2000, p. 37.
[5] GUPTA, A. K.—LLOYD, D. J.—COURT, S. A.: Mat. Sci. Eng., *A316*, 2001, p. 11.
[6] HIRTH, S. M.—MARSHALL, G. J.—COURT, S. A.—LLOYD, D. J.: Mat. Sci. Eng., *A319-321*, 2001, p. 452.
[7] ENGLER, O.—HIRSCH, J.: Mat. Sci. Eng., *A336*, 2002, p. 249.
[8] GUPTA, A. K.—LLOYD, D. J.—COURT, S. A.: Mat. Sci. Eng., *A301*, 2001, p. 140.
[9] EDWARDS, G. A.—STILLER, K.—DUNLOP, G. L.—COUPER, M. J.: Acta. Mater., *46*, 1998, p. 3893.
[10] MATSUDA, K.—SAKGUSHI, Y.—MIYATA, Y.—UTENI, Y.—SATO, T.—KAMIO, A.—IKENO, S.: J. Mater. Sci., *35*, 2000, p. 179.
[11] SHEGOLEVA, T. V.: Phys. Met. Metall., *25*, 1968, p. 56.
[12] CAYRON, C.—BUFFAT, P. A.: Acta Mater., *48*, 2000, p. 2639.
[13] MATSUDA, K.—GAMADA, H.—FUJI, K.—UTENI, Y.—SATO, T.—KAMIS, A.—IKENO, S.: Metall. Mater. Trans., *29A*, 1998, p. 1161.
[14] BIROL, Y.: ALUMINIUM, *80*, 2004, 1/2, p. 80.
[15] SLÁMOVÁ, M.—KARLÍK, M.—CIESLAR, M.—CHALUPA, B.—MERLE, P.: Kovove Mater., *39*, 2002, p. 389.
[16] SLÁMOVÁ, M.—KARLÍK, M.—CIESLAR, M.—CHALUPA, B.—MERLE, P.: Kovove Mater., *41*, 2003, p. 51.

Received: 26.4.2004